

Ocean Vector Winds Retrieval From C-Band Fully Polarimetric SAR Measurements

Biao Zhang, William Perrie, Paris W. Vachon, *Senior Member, IEEE*, Xiaofeng Li, William G. Pichel, Jie Guo, and Yijun He, *Member, IEEE*

Abstract—We present an efficient algorithm for retrieving the ocean-surface wind vector from C-band Radar Satellite RADARSAT-2 fully polarimetric synthetic aperture radar (SAR) measurements based upon the copolarized geophysical model function, i.e., CMOD5.N, and the cross-polarized ocean backscatter model, i.e., C-2PO. The analysis of fine quad-polarization mode single-look complex SAR data and collocated *in situ* moored buoy observations reveals that the polarimetric correlation coefficient between co- and cross-polarization channels has odd symmetry with respect to the wind direction. This characteristic is different from the feature that normalized radar cross sections for quad-polarization have even symmetry regarding the wind direction. We first use the C-2PO model to directly retrieve wind speeds without any external wind-direction and radar-incidence-angle inputs. Subsequently, the retrieved wind speeds, along with incidence angles and CMOD5.N, are employed to invert the wind direction, still with ambiguities. The odd-symmetry property is then applied to remove the wind direction ambiguities. Thus, it is shown that fully polarimetric SAR measurements provide complementary directional information for the ocean-surface wind fields. This method has the potential to improve wind vector retrievals from space.

Index Terms—Fully polarimetric SAR, ocean-surface wind fields, polarimetric correlation coefficient, SAR polarimetric odd-symmetry, simultaneous wind speed and direction SAR retrievals.

Manuscript received August 2, 2011; revised February 3, 2012; accepted March 17, 2012. Date of publication May 23, 2012; date of current version October 24, 2012. This work was supported in part by the Canadian Space Agency Government Related Initiatives Program project “Full polarization retrievals of ocean waves and winds,” by the National Nature Science Foundation of China project “Multi-frequencies polarimetric SAR wind field retrieval in coastal regions” (41176170), by the Nanjing University of Information Science and Technology High-Level Introduction of Talent project “Detection of marine oil spill by compact polarimetric SAR” (S8111003001), and by the National Natural Science Youth Foundation of Jiangsu Province “Remote sensing of ocean surface wind field by high-resolution fully polarimetric SAR” (SBK201241656). The views, opinions, and findings contained in this report are those of the authors and should not be construed as an official NOAA or U.S. Government position, policy, or decision.

B. Zhang and Y. He are with the School of Marine Sciences, Nanjing University of Information Science and Technology, Nanjing 210044, China.

W. Perrie is with the Fisheries and Oceans Canada, Bedford Institute of Oceanography, Dartmouth, NS B2Y 4A2, Canada (e-mail: William.Perrie@dfo-mpo.gc.ca).

P. W. Vachon is with the Defence Research and Development Canada—Ottawa, Ottawa, ON K1A 0Z4, Canada.

X. Li is with the I. M. Systems Group at National Oceanic and Atmospheric Administration/National Environmental Satellite, Data, and Information Service, Camp Springs, MD 20746 USA.

W. G. Pichel is with the National Oceanic and Atmospheric Administration/National Environmental Satellite, Data, and Information Service/Center for Satellite Applications and Research (STAR), Camp Springs, MD 20746 USA.

J. Guo is with Shandong Provincial Key Laboratory of Coastal Zone Environmental Processes, Yantai Institute of Coastal Zone Research, Chinese Academy of Sciences, Yantai 264003, China.

Digital Object Identifier 10.1109/TGRS.2012.2194157

I. INTRODUCTION

ACCURATE observations of surface winds over the oceans are required for a wide range of meteorological and oceanographic applications, since wind drives surface waves, provides initial conditions and verification data for numerical weather prediction, and serves as a basis for calculations of surface fluxes of heat, moisture, and momentum. Ocean surface winds from scatterometer observations can improve numerical weather prediction (NWP) model forecasts [1], [2]. While spaceborne scatterometry is useful and important for wind vector measurements on a global scale, the contamination from land reflections degrades scatterometer measurements in coastal regions [3]. In addition, the coarse resolution (25 km) of scatterometers also limits its applicability to investigate the variability of wind speed and wind direction on small scales.

Satellite synthetic aperture radar (SAR) sensors constitute an active microwave system that can provide subkilometer resolution ocean-surface wind data with large swath coverage (up to 500 km) and high resolution (25 or 50 m). Ocean surface wind retrieval from conventional single-polarization SAR backscatter measurements is achieved by using various geophysical model functions (GMFs) for X-, C-, and L-band SARs. Specifically for C-band, the commonly used GMFs are CMOD4 [4], CMOD_IFR2 [5], and CMOD5.N [6]. They are derived based on observations from spaceborne microwave scatterometers, which relate the VV-polarized normalized radar cross section (NRCS) of the ocean surface to the equivalent neutral wind speed at a 10-m height, the wind direction versus the antenna look direction, and the radar incidence angle. Over the last decade, single-frequency (C- or L-band) and single-polarization (VV or HH) SAR systems, e.g., Environmental Satellite (ENVISAT) Advanced Synthetic Aperture Radar (ASAR), Advanced Land Observing Satellite Phased Array type L-band Synthetic Aperture Radar, Radar Satellite RADARSAT-1, and RADARSAT-2, have been used to retrieve ocean-surface wind speeds with various GMFs and polarization-ratio models [7]–[12]. Since the two unknown parameters, i.e., wind speed and direction, simultaneously exist in the GMF, one must inevitably obtain the wind direction from external sources, prior to wind speed retrieval. Moreover, the copolarized backscatter is strongly dependent on the wind direction, and therefore, uncertainties in the wind direction can lead to significant errors in wind speed retrievals.

Generally, there are three approaches to obtain wind directions. The *first* method directly extracts wind directions from wind-induced streaks visible in the SAR image using fast Fourier transforms, local gradients, and wavelet analysis techniques [13]–[15]. Although this approach is often successful,

there are times when the windrow signature is weak or when there are other features in SAR images, such as oceanic or atmospheric internal waves, which can also produce linear features on the same spatial scale as that of wind rows. These nonwind-streak features are not generally aligned with the local wind vectors and can contaminate wind direction retrievals from the SAR image. In addition, the 180° directional ambiguities that exist in retrieved wind directions have to be removed by using wind shadows, weather charts, atmospheric models, buoy measurements, or ancillary data [7], [8]. The *second* method utilizes the wind direction estimates from global operational NWP models. This method has the following disadvantages: 1) NWP-model spatial resolutions are generally far less than those of the SAR images; and 2) NWP models tend not to include all aspects of marine atmospheric boundary layer physics necessary to resolve the fine-scale features observed by SAR [16]. The *third* method uses wind direction measurements from other operational sensors, i.e., scatterometer. As previously mentioned, scatterometer measurements suffer from accuracy loss in coastal regions [17]. The limitations in obtaining wind directions from these external sources are the main challenges for SAR wind speed retrieval.

Recently, C-band cross-polarized ocean backscatter has been documented as being insensitive to wind directions and radar incidence angles, and can be thus used to directly retrieve wind speeds [12], [18], [19]. This characteristic provides a potential opportunity to retrieve wind vectors with simultaneously acquired co- and cross-polarized SAR measurements.

In this paper, we present the result that the polarimetric correlation coefficient (PCC) between the VV and VH channels has odd symmetry with respect to wind direction. This characteristic is different from the NRCS values in quad-polarization (HH, HV, VH and VV), which have even symmetry with respect to wind direction. The odd symmetry property can be used to resolve the wind direction ambiguity. Following this rationale, we propose an efficient algorithm to simultaneously retrieve absolute wind speed and direction using C-band RADARSAT-2 fully polarimetric SAR data. In Section II, we describe the wind vector retrieval algorithm, followed by the wind direction ambiguity removal method in Section III. Discussions and conclusions are given in Section IV.

II. WIND VECTOR RETRIEVAL ALGORITHM

A. Wind Speed Retrieval

As previously mentioned, the ocean backscatter in co- and cross-polarizations are quite different; the latter is independent of wind direction and radar incidence angle but has a linear relationship with respect to wind speed. A C-band cross-polarized ocean backscatter model (C-2PO) relating NRCS in VH polarization σ_{VH}^o to the equivalent neutral wind speed at a 10-m height U_{10} was developed using RADARSAT-2 fine quad-polarization mode SAR data and collocated buoy observations, via a nonlinear least-square method [18], [20]. The C-2PO model is

$$\sigma_{VH}^o = 0.580 * U_{10} - 35.652 \quad (1)$$

where the units of σ_{VH}^o and U_{10} are in decibels and meters per second, respectively. Compared with a conventional copo-

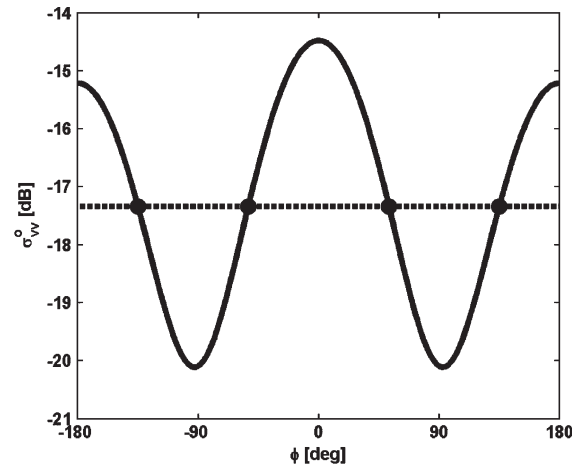


Fig. 1. (Black dots) All four relative wind direction solutions ϕ , $\pi - \phi$, $-\phi$, and $-(\pi - \phi)$ for the same NRCS in VV polarization (σ_{VV}^o) corresponding to an assumed wind speed of 10 m/s and an incidence angle of 45° , calculated by the CMOD5.N model. (Dashed line) Directional ambiguity of the model.

larized GMF, e.g., CMOD5.N [6], C-2PO is a straightforward mapping of calibrated cross-polarized NRCS to wind speed without *a priori* wind direction input. In comparisons with buoy wind speeds, the C-2PO model achieved a root mean square (RMS) error of 1.63 m/s, whereas CMOD5.N resulted in an RMS difference of 1.88 m/s [20]. It should be noted that C-2PO permits wind speed estimations only from observed C-band cross-polarized ocean backscatter that is sufficiently above the instrument noise floor (the noise-equivalent sigma naught or σ_{NE}^o), e.g., above 10 m/s for σ_{NE}^o of -30 dB or above 20 m/s for σ_{NE}^o of -25 dB [18]. According to RADARSAT-2 product documentation, the radiometric calibration error is less than 1 dB and σ_{NE}^o , for fine quad-polarization SAR data, i.e., -36.5 ± 3 dB [21].

B. Wind Direction Retrieval

Using wind speeds derived from the C-2PO model as input to the C-band copolarized GMF, i.e., CMOD5.N [6], we retrieve wind directions with ambiguities. CMOD5.N relates VV-polarized backscatter as sensed by the spaceborne ERS-2 and ASCAT scatterometers, to the equivalent neutral ocean vector wind at a 10-m height and scatterometer incidence angle. It takes the general form, i.e.,

$$\sigma_{VV}^o(\theta, U_{10}, \phi) = A_0(\theta, U_{10}) [1 + A_1(\theta, U_{10}) \cos \phi + A_2(\theta, U_{10}) \cos(2\phi)]^{1.6} \quad (2)$$

where θ , ϕ , and U_{10} are the incidence angle, the wind direction versus the antenna look direction (relative wind direction), and the wind speed, respectively. A_0 , A_1 , and A_2 are coefficients, which are dependent on the wind speed and the radar incidence angle. Fig. 1 illustrates the relative wind direction ϕ dependence of NRCS in VV polarization for ocean surfaces at a 45° incidence angle for 10-m/s wind speed. Fig. 1 also shows that VV-polarized NRCS values estimated from CMOD5.N have *even* symmetry with respect to the wind direction. For specific NRCS values in VV polarization and given wind speeds and incidence angles, there are four relative wind directions. If

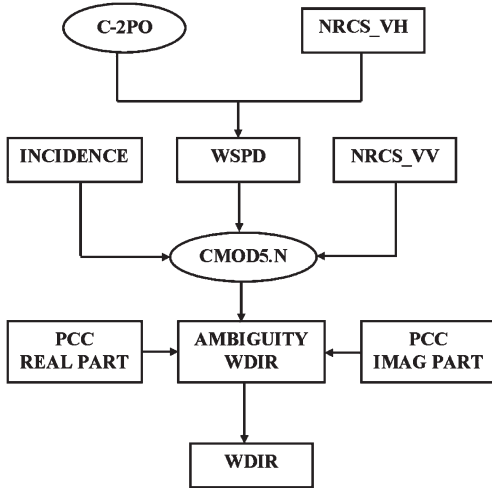


Fig. 2. Flowchart for the simultaneous wind speed and direction retrieval algorithm.

we use ϕ to represent one direction, the other three possible directions are $\pi - \phi$, $-\phi$, and $-(\pi - \phi)$.

In this paper, we propose a simultaneous wind speed and wind direction retrieval algorithm using CMOD5.N and C-2PO, the SAR-measured NRCS in VV and VH polarizations, and the radar incidence angle. Fig. 2 shows the flowchart for this wind vector retrieval method. The retrieved wind directions have the directional ambiguities previously noted, which can be resolved by using the different symmetric characteristics of PCC between the VV and VH channels and the NRCS values in quad-polarization. The former has *odd* symmetry with respect to the wind direction, whereas the latter has *even* symmetry. The details of removing the wind direction ambiguity solutions with PCC will be described in Section III.

III. WIND DIRECTION AMBIGUITY REMOVAL

A. Data Set

RADARSAT-2 fine quad-polarization mode single-look complex (SLC) SAR data are characterized by a nominal spatial resolution of $5.4 \text{ m} \times 8.0 \text{ m}$ in range and azimuth, respectively. For each individual quad-polarization SAR image with a specific beam mode, the pixel spacing in azimuth and range directions is about 5 m, respectively. The nominal incidence angles vary by about 1.5° across a swath of 25 km.

Before collocating quad-polarization SAR observations with buoy measurements, we first examine the homogeneity of the selected subsections of SAR images. It is well known that the wind speed can be only retrieved from SAR data that are free of sea-surface features *not* due to the local wind, e.g., sea ice and slicks. To exclude SAR images that contain features *not* associated with the local wind, a filter is applied. The filter was developed to distinguish between homogeneous and inhomogeneous SAR images and, furthermore, to retrieve ocean wave spectra and wind speed fields [22], [23]. This technique uses tests involving the statistical properties of periodograms, as commonly used for spectral estimations. According to the standard theory, spectral densities estimated from a single periodogram that are negative exponentially distributed have the basic property that variance $\text{var}(I)$ is equal the squared

mean intensity $\langle I \rangle^2$ [24]. Thus, we apply formula $\text{CVAR} = \text{var}(I)/\langle I \rangle^2$ to check the homogeneity of subsections of SAR images of about $100 \text{ m} \times 100 \text{ m}$ size. For a perfectly homogeneous image, the inhomogeneity parameter CVAR should be 1. Therefore, in the following discussion, all SAR images with an inhomogeneity parameter $\text{CVAR} \geq 1$ were defined as inhomogeneous. It should be mentioned that SAR images containing mesoscale oceanic or atmospheric phenomena are excluded from this analysis as inhomogeneous.

Subsequently, we make a 20 pixel \times 20 pixel boxcar average on the NRCS, in each polarization, so that the resampled pixel spacing is 100 m. To analyze the symmetry property between the PCC and the wind direction, we collected RADARSAT-2 fine quad-polarization mode SAR images from geographic locations that are collocated with 52 *in situ* National Oceanic and Atmospheric Administration (NOAA) National Data Buoy Center (NDBC) buoys located in the Gulf of Alaska, East and West coasts of the USA, and the Gulf of Mexico between December 2008 and May 2011. Each individual SAR image includes one NDBC buoy. The buoys' wind speeds and directions are averaged over 8-min periods. Buoy measurements also include hourly wave parameters (significant wave height, wave period, and wave direction) and surface meteorological parameters (air temperature, sea-surface temperature, dew point temperature, and sea-surface pressure). All buoy-measured wind speeds at different heights are converted to 10-m equivalent neutral wind conditions using the Tropical Ocean and Global Atmosphere Response Experiment (TOGA COARE) bulk flux algorithm (version 2.5) [25]. This algorithm is structured so as to derive the wind profiles and the roughness lengths using the buoy-measured values of air and sea-surface temperatures, dew point, air pressure, and wind speed. The buoy measurements and the RADARSAT-2 observations were required to occur within a time difference of 30 min. This matchup criterion resulted in a data set consisting of 1068 RADARSAT-2 observed NRCS (σ_{HH}^o , σ_{HV}^o , σ_{VH}^o , and σ_{VV}^o) estimates in quad-polarization mode and polarimetric scattering matrix elements (PSMEs) (S_{HH} , S_{HV} , S_{VH} , and S_{VV}), as well as radar incidence angles, collocated with buoy-measured wind speeds and wind directions. In this data set, the entire range of incidence angles and wind speeds are between 20° and 49° , and 1 and 26 m/s, respectively. Wind directions range from 0° to 360° .

B. Polarimetric Correlation Coefficient

Conventional SAR systems operate with a single fixed-polarization antenna for both transmission and reception of radio-frequency signals. In this way, a single scattering coefficient, namely, backscatter amplitude (intensity), is measured for a specific transmit-and-receive polarization combination. A result of this implementation is that the scattered wave, i.e., a vector quantity, is measured as a scalar quantity and any additional information about the scattering process contained in the polarization properties of the scattered signals is lost [26]. On the contrary, fully polarimetric SAR measures the complex scattering matrix of a given medium with quad-polarization and provides not only amplitude but also phase information associated with the reflectivity of all the scatterers contained in a resolution cell. The scattering matrix

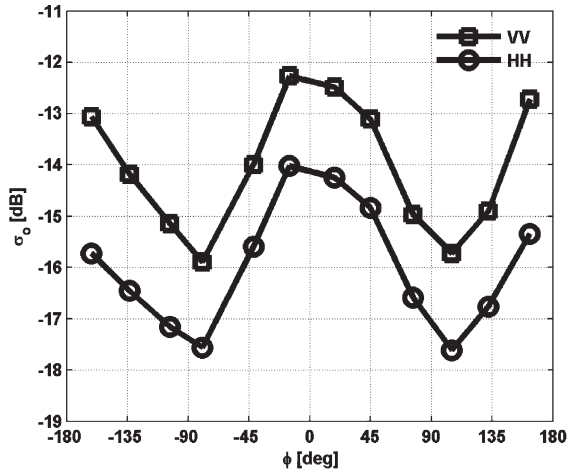


Fig. 3. RADARSAT-2 measured NRCS in VV and HH polarizations versus relative wind direction. The average wind speed and incidence angle are 10 m/s and 35°, respectively.

in a linear horizontal- and vertical-polarization base can be expressed as

$$S = \begin{bmatrix} S_{HH} & S_{HV} \\ S_{VH} & S_{VV} \end{bmatrix} \quad (3)$$

where S_{HV} is the scattering element of horizontal-transmitting and vertical-receiving polarization, and the other three elements are similarly defined. Each scattering matrix element is a complex number with its amplitude and phase indicating the strength of scattering signals and phase delay. The square of the absolute magnitude of each scattering matrix element represents the radar backscatter for each polarization. In addition to co- and cross-polarized backscatter measurements, fully polarimetric SAR can also acquire the correlation between different polarized backscatter measurements. The correlation between VV and VH polarization channels is denoted by PCC, i.e.,

$$\rho_{VVVH} = \frac{\langle S_{VV} \cdot S_{VH}^* \rangle}{\sqrt{\langle |S_{VV}|^2 \rangle \langle |S_{VH}|^2 \rangle}}. \quad (4)$$

This is a complex number that indicates the degree of correlation and relative phase angle (phase difference) of VV and VH polarized backscatter signals.

To analyze the symmetric characteristics of PCC with respect to wind direction, we first fixed the radar incidence angle and the wind speed as 35° and 10 m/s and thus obtained a small data set. Alternate examples, such as 25° and 15 m/s, would give similar results. The data set consists of PSMEs (S_{HH} , S_{HV} , S_{VH} , and S_{VV}) and NRCS (σ_{HH}^o , σ_{HV}^o , σ_{VH}^o , and σ_{VV}^o) in quad-polarizations. Subsequently, we combine collocated PSME with (4) to estimate PCC. Both NRCS in co- and cross-polarizations are shown to have even symmetry with respect to the wind direction in Figs. 3 and 4. We can also observe the upwind-to-downwind asymmetry of the NRCS that is induced by an additional nonpolarized contribution associated with breaking waves, which was explained in the literature using the composite Bragg model [27]. Figs. 5 and 6 show that the real and imaginary parts of PCC have odd symmetry with respect to wind direction. This observed odd symmetry of polarimetric active scattering, for satellite SAR,

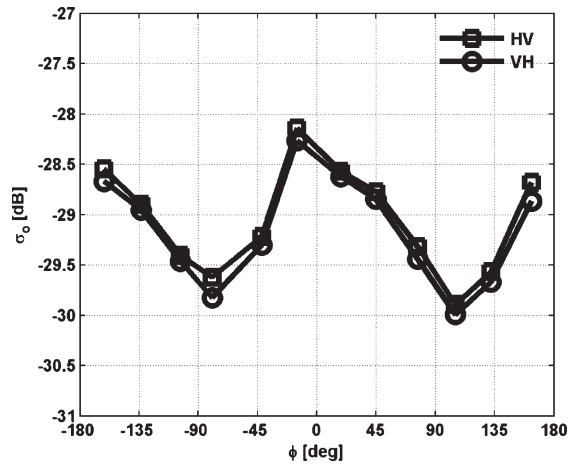


Fig. 4. RADARSAT-2 measured NRCS in HV and VH polarization versus relative wind direction. The average wind speed and incidence angle are 10 m/s and 35°, respectively.

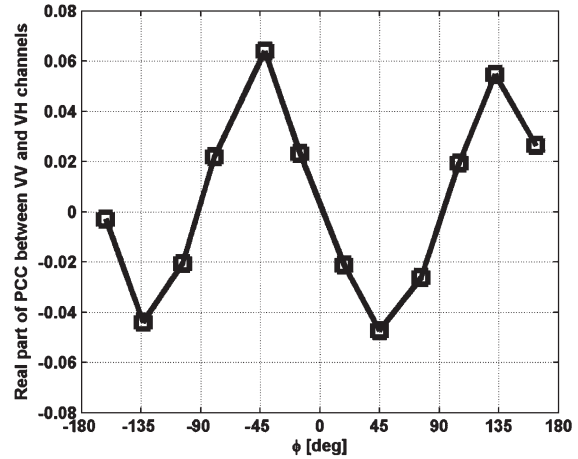


Fig. 5. RADARSAT-2 measured real part of the PCC between VV and VH channels versus relative wind direction. The average wind speed and incidence angle are 10 m/s and 35°, respectively.

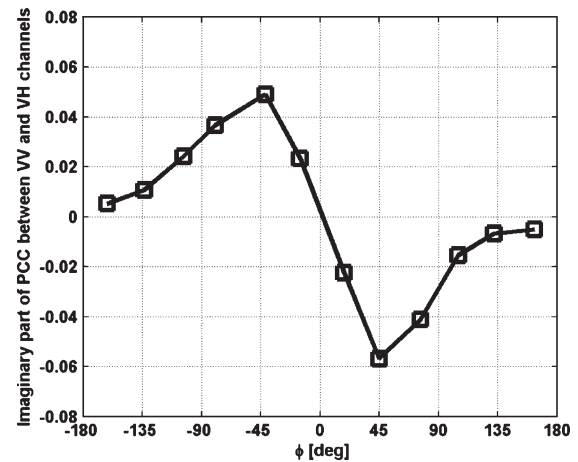


Fig. 6. RADARSAT-2 measured imaginary part of the PCC between VV and VH channels versus relative wind direction. The average wind speed and incidence angle are 10 m/s and 35°, respectively.

agrees with theoretical considerations from rigorous Maxwell equation derivations [28], two-scale models [29], and other earlier airborne polarimetric scatterometer observations [30],

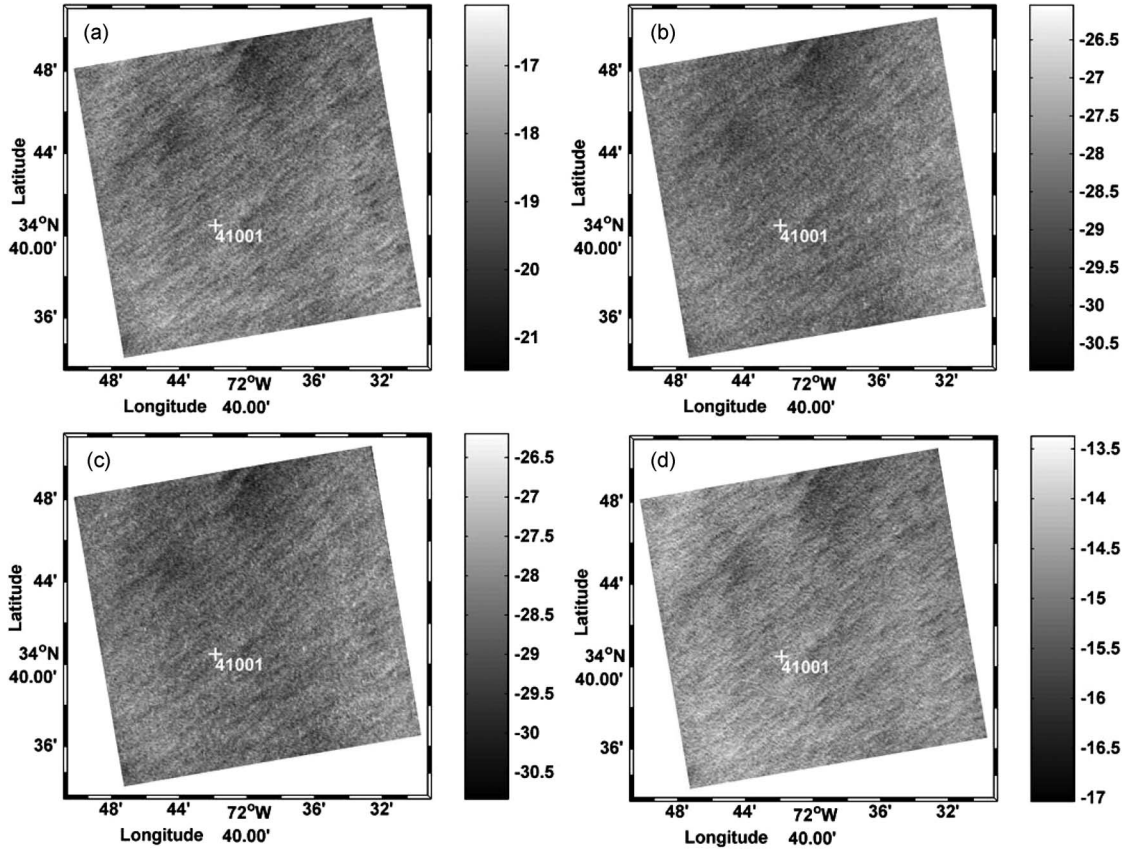


Fig. 7. C-band (a) HH-, (b) HV-, (c) VH-, and (d) VV-polarized SAR images off the U.S. East Coast from RADARSAT-2 fine quad-polarization mode SLC SAR data acquired on May 12, 2010, at 22:56 UTC (grayscale colorbar denotes sigma-naught; in units of decibels). NDBC buoy (#41001, $34^{\circ} 40' 30''\text{N } 72^{\circ} 41' 54''\text{W}$) is collocated to the SAR image. RADARSAT-2 Data and Product MacDonald, Dettwiler, and Associates Ltd., All Rights Reserved.abcd

[31]. The symmetry characteristic helps differentiate among the ambiguities separated by 180° .

We utilize PCC's odd symmetry characteristic to derive criteria to facilitate the selection of the relative wind direction among the four relative wind direction solutions, i.e., ϕ , $\pi - \phi$, $-\phi$, and $-(\pi - \phi)$. The criteria are as follows:

$$\begin{aligned} \text{If}(\text{PCC_Real} < 0 \ \& \ \text{PCC_Imag} > 0) \ \text{Then} \ -180^{\circ} < \Phi < -90^{\circ} \\ \text{If}(\text{PCC_Real} > 0 \ \& \ \text{PCC_Imag} > 0) \ \text{Then} \ -90^{\circ} < \Phi < 0^{\circ} \\ \text{If}(\text{PCC_Real} < 0 \ \& \ \text{PCC_Imag} < 0) \ \text{Then} \ 0^{\circ} < \Phi < 90^{\circ} \\ \text{If}(\text{PCC_Real} > 0 \ \& \ \text{PCC_Imag} < 0) \ \text{Then} \ 90^{\circ} < \Phi < 180^{\circ} \end{aligned}$$

where PCC_Real and PCC_Imag denote the real and imaginary parts of PCC, respectively.

In the following discussion, we first apply the proposed wind vector retrieval algorithm to three different sea state cases. Fig. 7 shows the first case, i.e., a RADARSAT-2 fine quad-polarization mode SAR image acquired on May 12, 2010, at 22:56 Coordinate Universal Time (UTC). This SAR image collocates with a NDBC buoy (#41001, $34^{\circ} 40' 30''\text{N } 72^{\circ} 41' 54''\text{W}$) off the U.S. East Coast. The buoy-measured 10-m equivalent neutral wind speed and direction are 13.3 m/s and 229° at 22:50 UTC. Fig. 8(a) shows the SAR-retrieved wind speeds from C-2PO and NRCS in VH polarization, on a 100-m resolution scale, without any external wind-direction and radar-incidence-angle inputs. The

resulting wind speed and incidence angle at each pixel were imported into CMOD5.N to estimate the wind direction, with ambiguities. Using the directional ambiguity removal criteria previously mentioned, the final wind directions are plotted in Fig. 8(b) without ambiguities. The SAR-retrieved wind speed and wind direction at the buoy location are 12.5 m/s and 213° . The second and third cases are quad-polarization images off the U.S. West Coast and in the Gulf of Alaska, which are shown in Figs. 9–11. The SAR-retrieved wind vectors are illustrated in Figs. 10 and 12. The comparisons between the wind vector retrievals of the two cases and buoy observations are summarized in Table I. It is shown that the SAR retrievals are in good agreement with buoy measurements, which suggests that the proposed simultaneous retrieval method for both wind speeds and wind directions is feasible for these three case studies.

Aside from specific case studies, we also made a statistical comparison. We randomly choose 534 (50% of the test data set) matchup pairs under different sea states to assess the proposed wind vector retrieval method. These pairs include the PSME, the NRCS in co- and cross-polarization modes, and buoy-measured wind speeds and wind directions. The cross-polarized backscatter and the C-2PO model are first used to directly retrieve wind speeds without wind-direction and incidence-angle inputs. The C-2PO retrieved wind speeds are found to be in good agreement with buoy observations, with a bias of 0.04 m/s and an RMS error of 1.39 m/s, as shown in Fig. 13(a). According to the C-2PO model (1), a calibration error of 1 dB

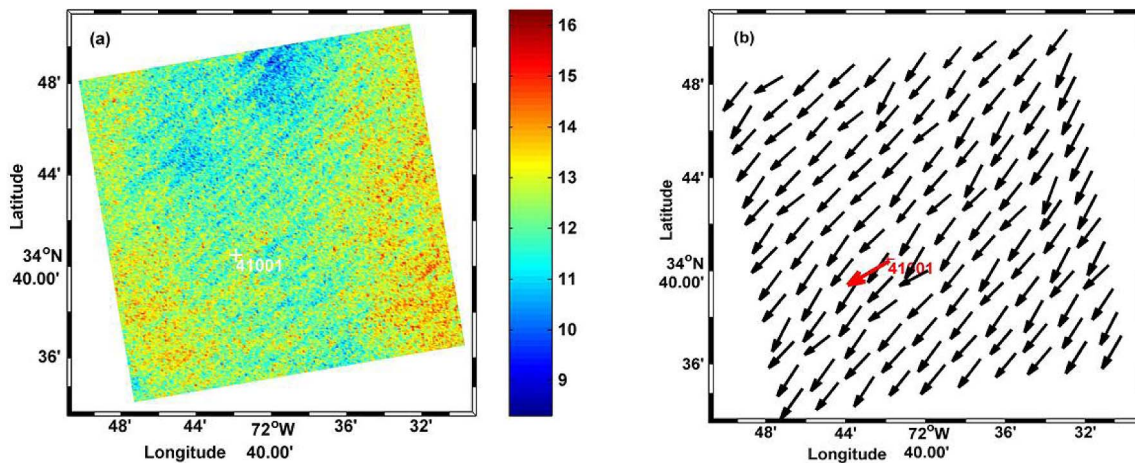


Fig. 8. (a) SAR-retrieved wind speeds from the C-2PO model and the VH-polarized SAR image, as shown in Fig. 7(c), without any external wind-direction and radar-incidence-angle inputs, and (b) SAR-retrieved wind directions without ambiguities from PCC between VV and VH channels, C-2PO-retrieved wind speeds, CMOD5.N, and VV-polarized SAR image, as shown in Fig. 7(d), as well as the radar incidence angle.

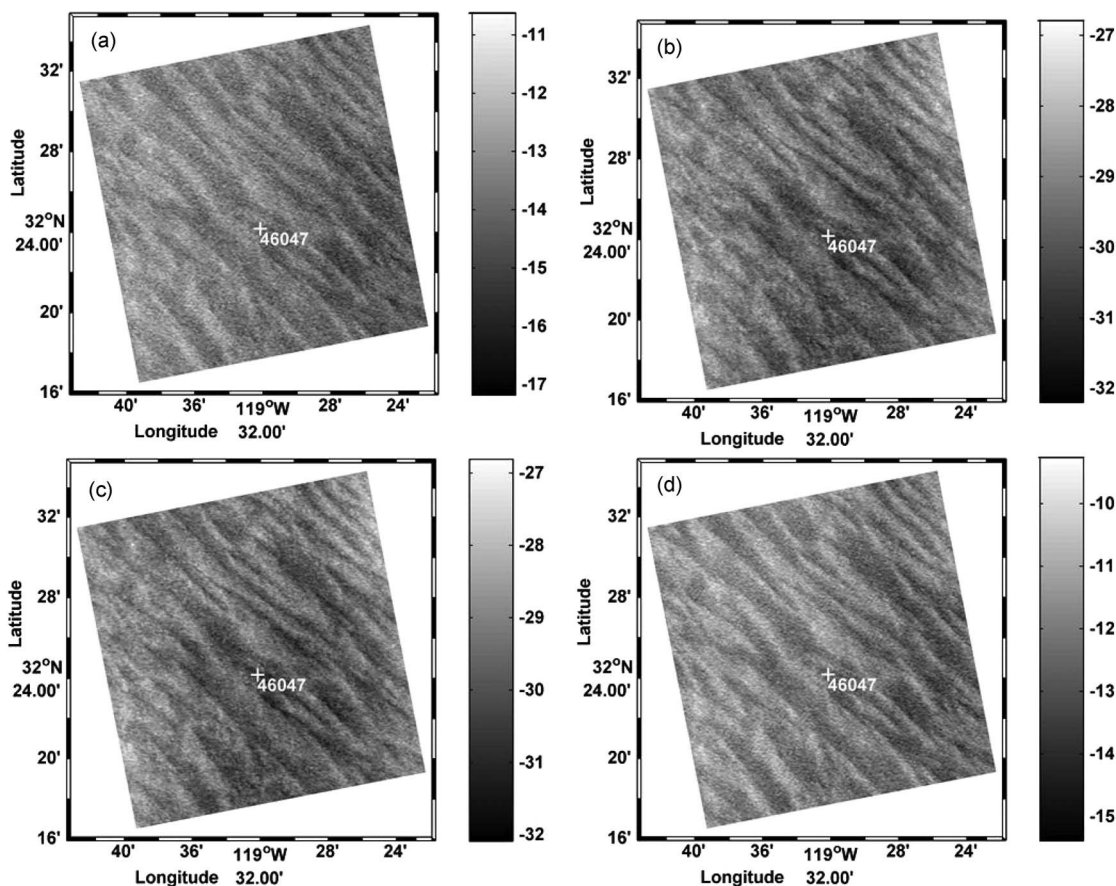


Fig. 9. C-band (a) HH-, (b) HV-, (c) VH-, and (d) VV-polarized SAR images off the U.S. West Coast from RADARSAT-2 fine quad-polarization mode SLC SAR data acquired on September 21, 2010, at 01:56 UTC (grayscale colorbar denotes sigma-naught; in units of decibels). NDBC buoy (#46047, 32° 24' 11'' N 119° 32' 08'' W) is collocated to the SAR image. RADARSAT-2 Data and Product MacDonald, Dettwiler, and Associates Ltd., All Rights Reserved.

in the cross-polarized NRCS will induce an error of 1/0.58 (1.72) m/s in the retrieved wind speed. Fig. 13(a) suggests the RADARSAT-2 quad-polarization SAR data have very good radiometric calibration. Under extreme weather conditions, the NRCS will be strongly dampened due to heavy-rain contam-

ination and additional effects associated with high waves and severe sea states, which are able to cause underestimation of the estimates for the highest wind speeds. Thus, rain effects on the NRCS have to be considered when retrieving wind speeds under intense rainfall environments [20].

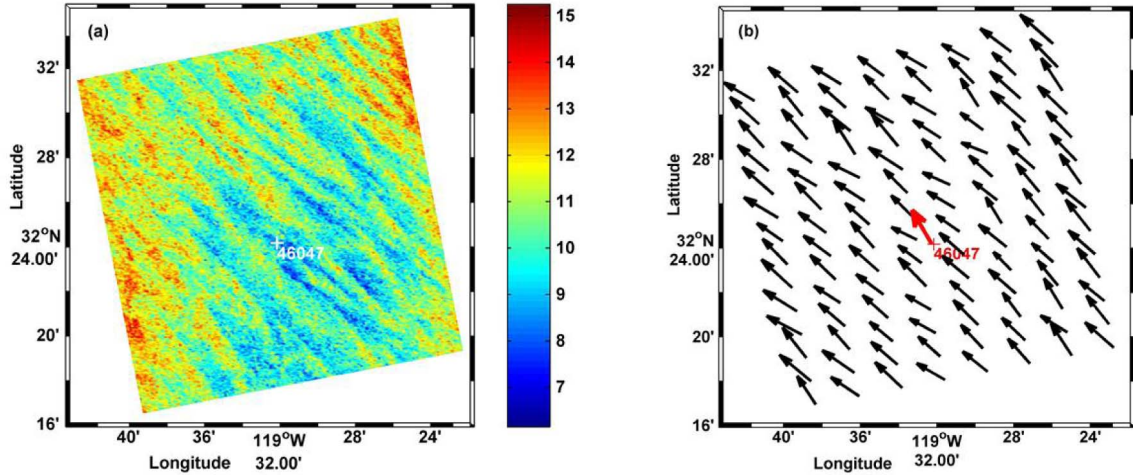


Fig. 10. (a) SAR-retrieved wind speeds from the C-2PO model and the VH-polarized SAR image, as shown in Fig. 9(c), without any external wind-direction and radar-incidence-angle inputs, and (b) SAR-retrieved wind directions without ambiguities from PCC between VV and VH channels, C-2PO-retrieved wind speeds, CMOD5.N, and VV-polarized SAR image, as shown in Fig. 9(d), as well as the radar incidence angle.

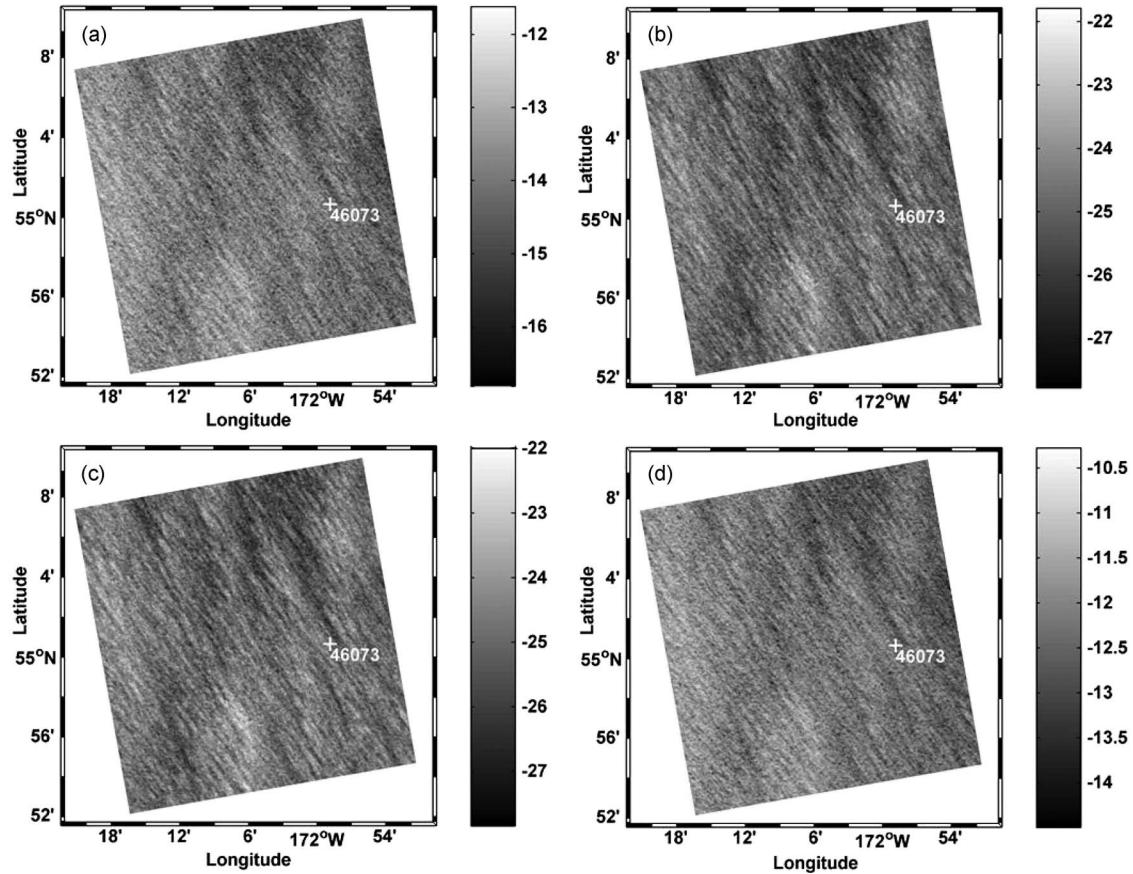


Fig. 11. C-band (a) HH-, (b) HV-, (c) VH-, and (d) VV-polarized SAR images off the Gulf of Alaska from RADARSAT-2 fine quad-polarization mode SLC SAR data acquired on January 9, 2011, at 05:15 UTC (grayscale colorbar denotes sigma-naught; in units of decibels). NDBC buoy (#46073, 55° 0' 40''N 171° 58' 50'' W) is collocated to the SAR image. RADARSAT-2 Data and Products© MacDonald, Dettwiler, and Associates Ltd. All Rights Reserved.

The resulting wind speeds from C-2PO and radar incidence angles are imported into CMOD5.N to estimate the wind directions. Using the criteria previously described, we removed all the wind direction ambiguities. Fig. 13(b) shows SAR-retrieved wind directions from CMOD5.N and PCC versus buoy-observed wind directions. The bias and the RMS error are 1.65° and 22.47°, respectively. The wind direction retrieval

errors come from two sources, i.e., inaccuracies in C-2PO and co- and cross-polarized NRCS calibration errors. Moreover, in high-wind conditions, NRCS dampening induced by rainfall may also be a factor. Fig. 13(c) shows SAR-retrieved wind speeds with sigma-naught in the VV polarization (σ_{VV}^0), using CMOD5.N and retrieved wind directions, versus C-2PO wind speeds. This result verifies that the retrieved wind directions

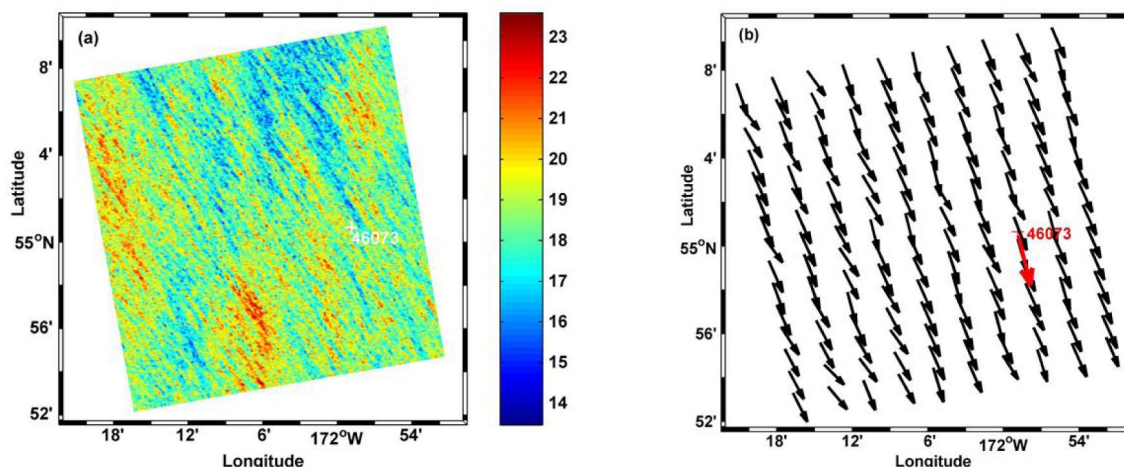


Fig. 12. (a) SAR-retrieved wind speeds from the C-2PO model and the VH-polarized SAR image, as shown in Fig. 11(c), without any external wind-direction and radar-incidence-angle inputs, and (b) SAR-retrieved wind directions without ambiguities from PCC between VV and VH channels, C-2PO-retrieved wind speeds, CMOD5.N, and VV-polarized SAR image, as shown in Fig. 11(d), as well as the radar incidence angle.

TABLE I
WIND SPEEDS AND DIRECTIONS RETRIEVED FROM THE THREE RADARSAT-2 FINE QUAD-POLARIZATION MODE SAR IMAGES COMPARED WITH CORRESPONDING WIND OBSERVATIONS PROVIDED BY NOAA NDBC BUOYS

Parameter	Case ID	Buoy ID	Retrieval	Buoy
Wave speed (m/s)	1	41001	13.3	12.5
	2	46047	11.1	10.3
	3	46073	17.8	19.0
Wind direction (degree)	1	41001	229	213
	2	46047	311	323
	3	46073	152	142

are good because the retrieved wind speeds from CMOD5.N are in good agreement with those of C-2PO, with a bias of -0.05 m/s and an RMS error of 1.84 m/s.

IV. DISCUSSION AND CONCLUSION

In this paper, we have presented a simultaneous wind speed and direction retrieval method based on RADARSAT-2 fine quad-polarization mode SLC SAR data. The cross-polarization backscatter model (C-2PO) and the NRCS in VH polarization have been used to directly retrieve the wind speed without any external wind-direction and radar-incidence-angle inputs. The resulting wind speeds from C-2PO and the NRCS in VV polarization, as well as incidence angles, are then imported into CMOD5.N to estimate the wind direction, with ambiguities.

We analyzed the quad-polarization SAR data with collocated *in situ* ocean-surface wind observations and found that the copolarized backscatters have *even* symmetry with respect to the wind direction, while the PCC between the co- and cross-

polarization channels has *odd* symmetry, with respect to the wind direction. This symmetry property can be used to remove the wind direction ambiguities. Three cases were used to show that it is feasible to derive ocean-surface vector wind images using the method proposed in this paper. To present a statistical assessment of the proposed wind vector retrieval algorithm, we randomly selected 534 SAR images collocated with buoy measurements, which represent 50% of our available data set of SAR and buoy matchups, under different sea states. We showed that the retrieved wind speeds and directions are in good agreement with buoy measurements. The retrieved wind speeds have essentially no bias (0.04 m/s) with an RMS error of 1.39 m/s. The corresponding retrieved wind directions have a small bias of 1.65° with an RMS error of 22.47° . These results indicate that fully polarimetric SAR measurements provide both wind speed and direction retrievals. When the retrieved wind directions are used in CMOD5.N to infer wind speeds, results verify well C-2PO wind speeds, with a bias of -0.05 m/s and an RMS error of 1.84 m/s.

The proposed vector-wind retrieval algorithm in this paper has been only tested with RADARSAT-2 fine quad-polarization mode SAR images, with small swath (25 km). For the monitoring of large oceanic areas, the fine mode domain is not practical. By comparison, the dual-polarization (VV, VH) ScanSAR wide mode SLC SAR data have large coverage (500 km). Moreover, the Canadian C-band RADARSAT Constellation Mission SAR satellites (to be launched in 2016) will provide SAR measurements in compact polarization mode with large swath (350 km) and medium resolution (50 m). These measurements can be transformed to quad-polarization values. Thus, the dual-polarization and compact-polarization imagery can potentially provide an operational technique for wind vector mapping with large area coverage.

ACKNOWLEDGMENT

The authors would like to thank the Canadian Space Agency for providing RADARSAT-2 fine quad-polarization mode single-look complex SAR imagery and NOAA for

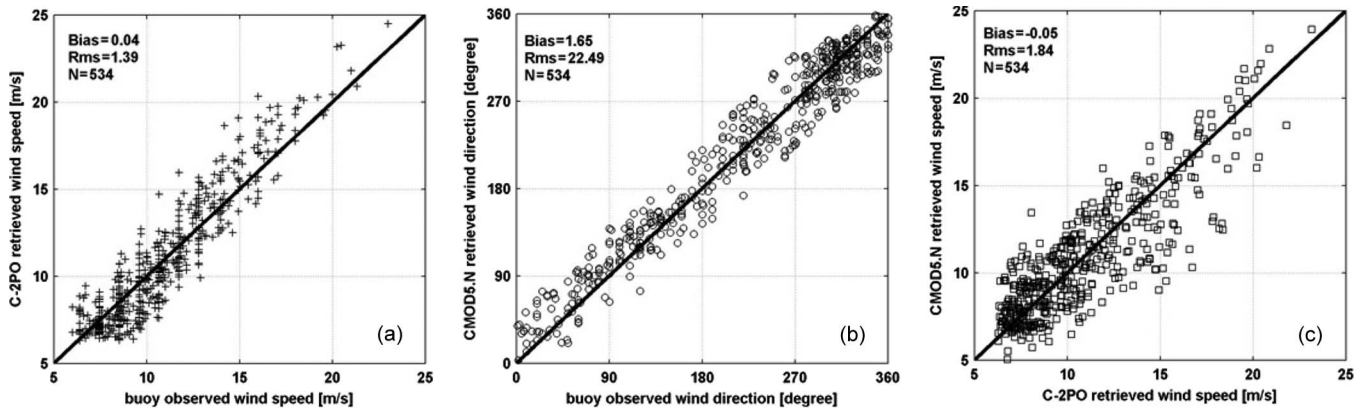


Fig. 13. (a) SAR-retrieved wind speeds from the C-2PO model and sigma-naught in the VH polarization (σ_{VH}^0) versus buoy-measured wind speeds, (b) SAR-retrieved wind directions without ambiguities from CMOD5.N and PCC versus buoy observed wind directions, and (c) SAR-retrieved wind speeds from CMOD5.N using sigma-naught in the VV polarization (σ_{VV}^0) and using retrieved wind directions versus C-2PO wind speeds.

supplying the buoy observations. The authors would also like to thank the two anonymous reviewers for helpful encouraging comments.

REFERENCES

- [1] R. Atlas, R. N. Hoffman, S. M. Leidner, J. Sienkiewicz, T.-W. Yu, S. C. Bloom, E. Brin, J. Ardizzone, J. Terry, D. Bungato, and J. C. Jusem, "The effects of marine winds from scatterometer data on weather analysis and forecast," *Bull. Amer. Meteorol. Soc.*, vol. 82, no. 9, pp. 1965–1990, Sep. 2001.
- [2] J. M. Von Ahn, J. M. Sienkiewicz, and P. S. Chang, "Operational impact of QuikSCAT winds at the NOAA ocean prediction center," *Weather Forecasting*, vol. 21, no. 4, pp. 523–539, Aug. 2006.
- [3] X. Yang, X. Li, W. G. Pichel, and Z. Li, "Comparison of ocean-surface winds retrieved from QuikSCAT scatterometer and RADARSAT-1 SAR in offshore waters of the US west coast," *IEEE Geosci. Remote Sens. Lett.*, vol. 8, no. 1, pp. 163–167, Jan. 2011.
- [4] A. Stoffelen and D. Anderson, "Scatterometer data interpretation: Estimation and validation of the transfer function CMOD4," *J. Geophys. Res.*, vol. 102, no. C3, pp. 5767–5780, 1997.
- [5] Y. Quilfen, B. Chapron, T. Elfohaily, K. Katsaros, and J. Tournadre, "Observation of tropical cyclones by high-resolution scatterometry," *J. Geophys. Res.*, vol. 103, no. C4, pp. 7767–7788, Apr. 1998.
- [6] H. Hersbach, "Comparison of C-band scatterometer CMOD5.N equivalent neutral winds with ECMWF," *J. Atmos. Ocean. Technol.*, vol. 27, no. 4, pp. 721–736, Apr. 2010.
- [7] J. Horstmann and W. Koch, "Measurement of ocean surface winds using synthetic aperture radars," *IEEE J. Ocean. Eng.*, vol. 30, no. 3, pp. 508–515, Jul. 2005.
- [8] Y. He, W. Perrie, Q. Zou, and P. W. Vachon, "A new wind vector algorithm for C-band SAR," *IEEE Trans. Geosci. Remote Sens.*, vol. 43, no. 7, pp. 1453–1458, Jul. 2005.
- [9] T. Shimada, H. Kawamura, and M. Shimada, "An L-band geophysical model function for SAR wind retrieval using JERS-1 SAR," *IEEE Trans. Geosci. Remote Sens.*, vol. 41, no. 3, pp. 518–531, Mar. 2003.
- [10] P. W. Vachon and F. W. Dobson, "Wind retrieval from RADARSAT SAR images: Selection of a suitable C-band HH polarization wind retrieval model," *Can. J. Remote Sens.*, vol. 26, pp. 306–313, 2000.
- [11] F. M. Monaldo, D. R. Thompson, W. G. Pichel, and P. Clemente-Colón, "A systematic comparison of QuikSCAT and SAR ocean surface wind speeds," *IEEE Trans. Geosci. Remote Sens.*, vol. 42, no. 2, pp. 283–291, Feb. 2004.
- [12] B. Zhang, W. Perrie, and Y. He, "Wind speed retrieval from RADARSAT-2 quad-polarization images using a new polarization ratio model," *J. Geophys. Res.*, vol. 116, no. C8, p. C08008, 2011, DOI: 10.1029/2010JC006522.
- [13] S. Lehner, J. Horstmann, W. Koch, and W. Rosenthal, "Mesoscale wind measurements using recalibrated ERS SAR images," *J. Geophys. Res.*, vol. 103, no. C4, pp. 7847–7856, Apr. 1998.
- [14] W. Koch, "Directional analysis of SAR images aiming at wind direction," *IEEE Trans. Geosci. Remote Sens.*, vol. 42, no. 4, pp. 702–710, Apr. 2004.
- [15] Y. Du, P. W. Vachon, and J. Wolfe, "Wind direction estimation from SAR images of the ocean using wavelet analysis," *Can. J. Remote Sens.*, vol. 28, no. 3, pp. 498–509, Jun. 2002.
- [16] X. Li, W. Zheng, X. Yang, Z. Li, and W. Pichel, "Sea surface imprints of coastal mountain lee waves imaged by SAR," *J. Geophys. Res.*, vol. 116, p. C02014, 2011, DOI: 10.1029/2010JC006643.
- [17] X. Yang, X. Li, W. G. Pichel, and Z. Li, "Comparison of ocean surface winds from ENVISAT ASAR, MetOp ASCAT scatterometer, buoy measurements and NOGAPS model," *IEEE Trans. Geosci. Remote Sens.*, vol. 49, no. 12, pp. 4743–4750, Dec. 2011.
- [18] P. W. Vachon and J. Wolfe, "C-band cross-polarization wind speed retrieval," *IEEE Geosci. Remote Sens. Lett.*, vol. 8, no. 3, pp. 456–459, May 2011.
- [19] P. A. Hwang, B. Zhang, J. V. Toporkov, and W. Perrie, "Comparison of composite Bragg theory and quad-polarization radar backscatter from RADARSAT-2: With applications to wave breaking and high wind retrieval," *J. Geophys. Res.*, vol. 115, p. C08019, 2010, DOI:10.1029/2009JC005995.
- [20] B. Zhang and W. Perrie, "Cross-polarized synthetic aperture radar: A potential measurement technique for hurricanes," *Bull. Amer. Meteorol. Soc.*, vol. 93, no. 4, pp. 531–541, Apr. 2012.
- [21] B. Slade, *RADARSAT-2 Product Description*. Issue 1/6, RN-SP-52-1238. [Online]. Available: http://gs.mdacorporation.com/products/sensor/radarsat2/RS2_Product_Description.pdf
- [22] S. Lehner, J. Schulz-Stellenfleth, B. Schättler, H. Breit, and J. Horstmann, "Wind and wave measurements using complex ERS SAR wave mode data," *IEEE Trans. Geosci. Remote Sens.*, vol. 38, no. 5, pp. 2246–2257, Sep. 2000.
- [23] J. Horstmann, H. Schiller, J. Schulz-Stellenfleth, and S. Lehner, "Global wind speed retrieval from SAR," *IEEE Trans. Geosci. Remote Sens.*, vol. 41, no. 10, pp. 2277–2286, Oct. 2003.
- [24] J. Honerkamp, *Stochastic Dynamical Systems*. Berlin, Germany: VCHVerlagsge-sellschaft mbH, 1993.
- [25] C. W. Fairall, E. F. Bradley, D. P. Rogers, J. B. Edson, and G. S. Yong, "Bulk parameterization of air-sea fluxes for tropical ocean global atmosphere coupled ocean-atmosphere response experiment," *J. Geophys. Res.*, vol. 101, no. C2, pp. 3747–3764, 1996, DOI:10.1029/95JC03205.
- [26] J. J. Van Zyl, "Unsupervised classification of scattering behavior using radar polarimetry data," *IEEE Trans. Geosci. Remote Sens.*, vol. 27, no. 1, pp. 36–45, Jan. 1989.
- [27] A. A. Mouche, D. Hauser, and V. Kudryavtsev, "Radar scattering of the ocean surface and sea-roughness properties: A combined analysis from dual-polarizations airborne radar observations and models in C-band," *J. Geophys. Res.*, vol. 111, p. C09004, 2006, DOI: 10.1029/2005JC003166.
- [28] S. H. Yueh, R. Kwok, and S. V. Nghiem, "Polarimetric scattering and emission properties of targets with reflection symmetry," *Radio Sci.*, vol. 29, no. 6, pp. 1409–1420, 1994.
- [29] S. H. Yueh, "Modeling of wind direction signals in polarimetric sea surface brightness temperatures," *IEEE Trans. Geosci. Remote Sens.*, vol. 35, no. 6, pp. 1400–1418, Nov. 1997.

- [30] W.-Y. Tsai, S. V. Nghiem, J. N. Huddleston, M. W. Spencer, B. W. Stiles, and R. D. West, "Polarimetric scatterometry: A promising technique for improving ocean surface wind measurements from space," *IEEE Trans. Geosci. Remote Sens.*, vol. 38, no. 4, pp. 1903–1921, Jul. 2000.
- [31] S. H. Yueh, W. J. Wilson, and S. Dinardo, "Polarimetric radar remote sensing of ocean surface wind," *IEEE Trans. Geosci. Remote Sens.*, vol. 40, no. 4, pp. 793–800, Apr. 2002.



Biao Zhang received the B.S. degree in surveying and mapping engineering from the China University of Petroleum, Shandong, China, in 2003 and the Ph.D. degree in physical oceanography from the Chinese Academy of Sciences, Qingdao, China, in 2008.

From 2008 to 2011, he was a Postdoctoral Fellow in a Canadian Government Laboratory with Bedford Institute of Oceanography, Dartmouth, NS, Canada. During this period, he won the Visiting Fellowship Scholarship of the Natural Sciences and Engineering

Research Council of Canada. Since November 2011, he has been a Professor with the School of Marine Sciences, Nanjing University of Information Science and Technology, Nanjing, China. His research interests include interferometric and polarimetric SAR ocean wave and wind algorithm development, marine oil-spill detection, investigation of extremely oceanic weather, and observation of mesoscale cellular convection and sea-surface thermal fronts using spaceborne multisensors.



William Perrie received the B.S. degree in physics from the University of Toronto, Toronto, ON, Canada, in 1973 and the Ph.D. degree in meteorology and oceanography from the Massachusetts Institute of Technology, Cambridge, in 1979.

He was a Postdoctoral Fellow in oceanography and mathematics with the University of British Columbia, Vancouver, BC, Canada, and the National Center for Atmospheric Research. He is currently a Senior Scientist with the Bedford Institute of Oceanography, Dartmouth, NS, Canada, and an

Adjunct Professor with Dalhousie University, Halifax, NS, Canada. His research interests are modeling of ocean wave, air–sea fluxes, coupled atmosphere–ocean interactions, and impacts of climate change on these variables, and field measurements, via remote sensing and *in situ*, of winds, waves, and currents.



Paris W. Vachon (M'89–SM'96) received the B.Ap.Sc (honors) degree in engineering physics and the Ph.D. degree in physical oceanography from the University of British Columbia, Vancouver, BC, Canada, in 1983 and 1987, respectively.

From 1987 to 1988, he was a Visiting Fellow in a Canadian Government Laboratory with the Canada Centre for Remote Sensing (CCRS) and the Radar Satellite Project Office, Ottawa, ON, Canada. In 1988, he was a Research Scientist with CCRS. From 1993 to 1994, he was a Visiting Scientist

with Nansen Environmental and Remote Sensing Center, Bergen, Norway. In 2002, he became the Head of CCRS's Harsh Environment Applications Sections. Since 2003, he has been with the Defence Research and Development Canada–Ottawa, Ottawa, where he is leading the Radar Data Exploitation Group. His research interests include many aspects of SAR ocean imaging including ship detection, ocean wind and wave retrieval, and storms such polar lows and hurricanes. He was the Editor-in-chief of the *Canadian Journal of Remote Sensing* from 1999 to 2003.

Dr. Vachon is an Associate Fellow of the Canadian Remote Sensing Society.



Xiaofeng Li received the B.S. degree in optical engineering from Zhejiang University, Hangzhou, China, in 1985, the M.S. degree in physical oceanography from the State Oceanic Administration of China, Beijing, China, in 1992, and the Ph.D. degree in physical oceanography from North Carolina State University, Raleigh, in 1997.

From 1985 to 1992, he studied and worked with the First Institute of Oceanography, State Oceanic Administration of China. Since 1997, he has been with the National Oceanic and Atmospheric Administration/National Environmental Satellite, Data, and Information Service

(NESDIS), Camp Springs, MD. His research interests include remote-sensing observation and theoretical/numerical model studies of various types of oceanic and atmospheric phenomena, image processing, ocean-surface oil spill and target detection with multipolarization synthetic aperture radar, and sea-surface temperature algorithm development. He is also involved in developing many operational satellite ocean remote-sensing products with NESDIS.



William G. Pichel received the B.S. degree in physics from the University of Florida, Gainesville, in 1969 and the M.S. degree in physical oceanography from the University of Hawaii, Honolulu, in 1979.

Since 1970, he has been with the National Oceanic and Atmospheric Administration/National Environmental Satellite, Data, and Information Service (NESDIS), Camp Springs, MD. He was the Product Area Leader for Oceanographic Products and the Chief of the Product Systems Branch. Since 1988,

he has been a Physical Scientist with the Satellite Oceanography and Climatology Division, Center for Satellite Applications and Research (STAR), NOAA/NESDIS, where he is the Chair of the Sea Surface Roughness Science Team and the NESDIS Point of Contact to the NOAA Marine Debris Program. His research interests include the development of ocean and hydrologic applications of SAR data and the improvement of sea-surface temperatures (SST) from satellite infrared measurements.

Mr. Pichel is a recipient of four Department of Commerce Bronze Medals for his work in SST and SAR and one Silver Medal for his work in marine debris detection at sea.



Jie Guo received the B.S. degree in applied mathematics and the M.S. degree in physical oceanography from the Ocean University of China, Qingdao, China, in 2002 and 2006, respectively, and the Ph.D. degree in physical oceanography from the Chinese Academy of Sciences, Qingdao, in 2009.

Since July 2009, she has been with the Yantai Institute of Coastal Zone Research, Chinese Academy of Sciences. Her research interests include ocean waves and sea-surface wind remote sensing, as well as marine oil pollution detection by multipolarization

synthetic aperture radar.



Yijun He (M'03) received the B.S. degree in physics from Hunan Normal University, Changsha, China, in 1985, the M.S. degree in applied physics from Xidian University, Xi'an, China, in 1990, and the Ph.D. degree in microwave theory and technology from Southeast University, Nanjing, China, in 1993.

He was with the Key Laboratory of Ocean Circulation and Waves, Institute of Oceanology, Chinese Academy of Sciences, where he was the Head of the Remote Sensing Group and Senior Scientist in satellite oceanography from 1999 to 2011. From 1993 to

1996, he was a Postdoctoral Fellow with the Ocean Remote Sensing Institute, Ocean University of China. He was a Visiting Scientist with the University of Hamburg, Hamburg, Germany, with the Bedford Institute of Oceanography, Dartmouth, NS, Canada, and with the University of Delaware, Newark. He is currently a Professor of ocean remote sensing and the Dean of the School of Marine Sciences with the Nanjing University of Information Science and Technology, Nanjing, China. His research interests include ocean waves, sea-surface wind speed, and other ocean-surface features related to remote sensing by fully polarization synthetic aperture radar and other microwave radar at low incidence angle, air–sea gas exchange using microwave remote sensing and numerical model, and sea-surface scattering of electromagnetic waves.